UDC 669.296:621.793

VACUUM-ARC CHROMIUM COATINGS FOR Zr-1Nb ALLOY PROTECTION AGAINST HIGH-TEMPERATURE OXIDATION IN AIR

A.S. Kuprin, V.A. Belous, V.V. Bryk, R.L. Vasilenko, V.N. Voyevodin, V.D. Ovcharenko, G.N. Tolmachova, I.V. Kolodiy, V.M. Lunyov, I.O. Klimenko
National Science Center "Kharkov Institute of Physics and Technology", Kharkov, Ukraine
E-mail: kuprin@kipt.kharkov.ua

The effect of vacuum-arc Cr coatings on the alloy E110 resistance to the oxidation in air at temperatures 1020 °C and 1100 °C for 3600 s has been investigated. The methods of scanning electron microscope, X-ray analysis and nanoindentation were used to determine the thickness, phase, mechanical properties of coatings and oxide layers. The results show that the chromium coating can effectively protect fuel tubes against high-temperature oxidation in air for one hour. In the coating during oxidation at T = 1100 °C a Cr_2O_3 oxide layer of 5 μm thickness is formed preventing further oxygen penetration into the coating, and thus the tube shape is conserved. Under similar test conditions the oxidation of uncoated tubes with formation of a porous monocline oxide of ZrO_2 of a thickness more than ≥ 250 μm is observed, then the deformation and cracking of samples occur and the oxide layer breaks away.

INTRODUCTION

A base material of fuel cladding in WWER-type reactors is Zr alloy with 1% of Nb (Zr-1Nb). This alloy possesses a high corrosion resistance under in-reactor conditions at temperatures of 350 °C. However, under accident conditions, accompanied by a sharp raise of temperature, this cladding material does not provide a reliable fuel protection against the contact with a coolant. In air the oxidation of zirconium elements occurs more intensively than in flowing steam because of nitrogen assistance accelerating the degradation of protective properties of the oxide film on zirconium [1, 2]. Therefore, the problem of fuel element protection against high-temperature oxidation in steam, as well as in air, is of current importance. Mechanisms of high-temperature oxidation in various media of zirconium alloys and anticorrosive methods are under consideration in many research papers [1–13]. PVD methods for deposition of protective heat-resistant coatings are used to increase effectively the oxidation resistance [10–13]. The choice of chromium, as a protective coating, is due to its exclusively high oxidation stability [14]; high heat conduction (93.9 W/мK), low activation capacity and low cross section of thermal neutron capture (3.05 barn).

It is well known [15] that gas-thermal chromium coatings are highly air oxidation- resistant at temperatures up to 1100 °C. Chromium layers of 4…5 μm thickness substantially decrease the oxidation rate of pure zirconium in water at 350 °C [10]. Oxidation experiments conducted in flowing steam at 1000 °C for 15000 s with samples of Zry-4 alloy having a PVD chromium coating showed a sharp decrease of oxidation kinetics and hydrogen concentration as compared to the uncoated alloy [12]. Paper [16] reports positive results of tests with UO_2-Cr dispersion fuel (oxide particles in chromium cladding for high-temperature fast neutron reactors) in water and in steam in the temperature range of 350…600 °C and pressure of 6…15 MPa, as well as, in gaseous medium (oxygen, nitrine) at temperatures of 20…800 °C. It has been established that the fuel developed provides a reliable operating efficiency of fuel elements in both the thermal reactor and the fact reactor up to burnup more than 10%.

The purpose of this study was to determine the influence of vacuum-arc chromium coatings on the oxidation of zirconium and zirconium alloys in air at temperatures of 1020 and 1100 °C. The choice of test temperatures depends on the zirconium alloy behavior peculiarities in this temperature range. According to the Zr-Nb system state diagram these temperatures correspond to1020 °C above the (α+β) ↔β transition and to 1100 °C in the β-phase region [17].

1. EXPERIMENTAL PROCEDURE

Chromium coatings were deposited by the vacuum-arc method from the two counter flows of metallic plasma with planetary rotation of samples on the system axis [18]. Chromium (99.9%) was used as cathodes. The temperature of samples during deposition did not exceed 500 °C. The initial vacuum in the system was at a level $P_0 \approx 7 \cdot 10^{-4}$ Pa. The coating thickness was ≈ 6…8 μm.

The samples were segments (length 10 mm, outer diameter 9.2 mm, wall thickness 0.7 mm) cut from the alloy E110 cladding tube. To measure the nanohardness and to perform X-ray analysis of condensates the coatings were also deposited onto the iodide zirconium disks of 15 mm diameter and 1.5 mm thickness. Coatings were deposited onto the outer tube surface and on one of the disk sides.

The chromium condensate structure was investigated by the methods of transmission electron microscopy with a JEM 100CX microscope. Diffractometry of samples was carried out with a diffractometer DRON-4-07 in Cu-Kα radiation using a selectively-absorbing nickel filter. The radiation diffracted from the samples was recorded with a scintillation detector. The phase composition, structure parameters and substructure characteristics were determined by the Rietveld method (MAUD software). Silicon powder was used to determine the crystalline size and the microstress level to take into account an instrumental line spreading as a standard. The tube nanohardness (H) was measured with a device Nanoindentor G200. The data processing was

performed by the Oliver and Pharr method [19] at a fixed depth of indenter penetration of 500 nm. Indentation was performed on the transverse metallographic sections from tubes. The spread of values did not exceed 10%.

High-temperature oxidation tests of samples were done by annealing them in the furnace with ohmic heating in air for 3600 s. Tubes were placed into the furnace after a required temperature has been reached. The heating rate was of about 20 °C/s and the cooling rate was of about 5 °C/s. The samples after testing were photographed. Investigations were carried out on the tube metallographic cross sections cut from the middle part of samples before and after oxidation. On the metallographic sections the outer tube side is coated and the inner tube side is uncoated. The thickness of coatings and that of oxide layer, as well as, the oxygen penetration depth from the outer and inner tube edges were measured by the scanning electron microscopy and energy-dispersion analysis of elements with a JSM-7001F device.

2. RESULTS AND DISCUSSION

By appearance the as-received vacuum-arc coatings are dense, solid, smooth (the roughness is not higher than the initial roughness of the zirconium tube ~ 0.7 μm), grey condensates. The photography of the Cr-coated tube and the electron microscopic image of its transverse metallographic section are shown in Fig. 1. The coating thickness is ~ 6.5 μm (Fig. 1,b). According to nanoindention data the hardness of as-received zirconium is at a level of ~ 2 GPa and the Young module is ~ 110 GPa. The Cr coating has a hardness of 4 GPa and the Young module ~ 300 GPa that is slightly higher than the values of bulk chromium [14]. Such an increase in hardness is characteristic for chromium vacuum-arc condensates due to their fine-crystalline structure and presence in them of residual compression stresses. Fig. 2 presents the TEM micrograph of the vacuum-arc chromium coating structure and the electron diffraction pattern and histogram of coating grain size distribution.

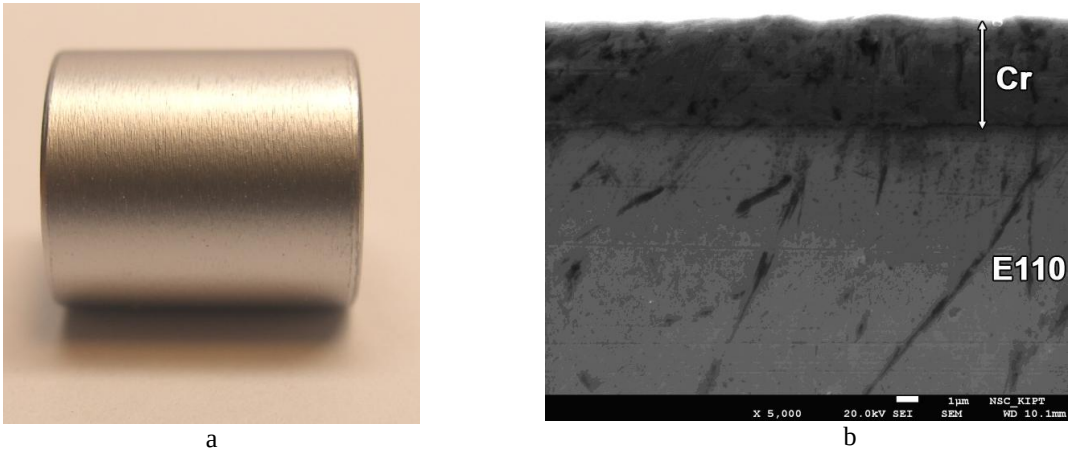

a b

Fig. 1. Photograph of the E110 tube with chromium coating (a) and SEM image of tube metallographic section (b)

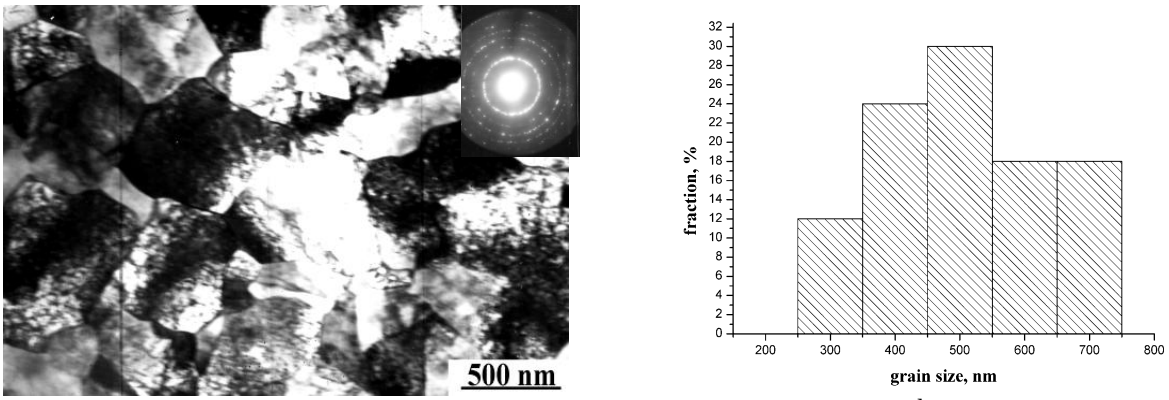

a b

Fig. 2. TEM micrographs of the Cr coating structure (a) and histogram of coating grain size distribution (b)

It is seen from the figure that the deposited chromium condensate has a fine-crystalline structure with an average grain size of ~ 450 nm. The diffraction patterns of chromium films include texture maxima, which look as points, indicating on the oriented growth of some grains. Besides the points there are texture maxima in the form of small arcs which evidence on the presence of grains of a random orientation.

Fig. 3,a shows the diffraction patterns of uncoated zirconium samples. In the initial iodide zirconium sample only the α-Zr phase is observed. Its parameters are: $a=3{,}238\pm1\cdot10^{-3}$ Å, $c=5{,}150\pm2\cdot10^{-3}$ Å. These values are higher than the corresponding literature data (a=3.232 Å, c=5.147 Å) that indicates on the impurity presence in the sample. Most probably it is oxygen (~0.5 wt.%). The line intensity distribution shows that the sample contains a texture, the crystallographic plane (002) of approximately 45% of grains is oriented in parallel to the sample plane.

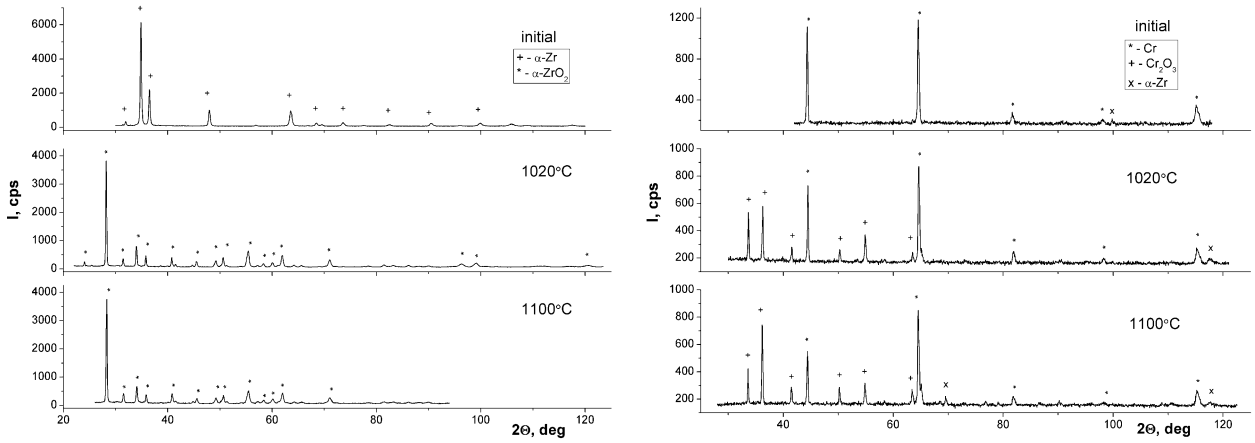

a b

Fig. 3. Diffraction patterns of uncoated zirconium samples (a) and of chromium coated samples (b) before and after oxidation at temperatures 1020 °C and 1100 °C

In the initial sample with coating (Fig. 3,b) only a Cr phase is observed. The chromium lattice parameter is $a = 2.8847 \pm 2 \cdot 10^{-4}$ Å. The crystalline size of this phase is $D = (214 \pm 12)$ nm and the microstresses level is $\varepsilon = 8{,}1 \cdot 10^{-4}$. As is shown by the line intensity distribution there is a texture (200) in the sample. A degree of texturing (fraction of grains oriented by the preset plane in parallel with the sample surface) is 66%. For all the samples with deposited Cr coating on the diffraction patterns at wide angles ($2\theta \geq 70°$) the substrate marks of the α-Zr phase were observed. It is related with a nonlinear dependence of the X-ray penetration depth on the diffraction angle (at $2\theta = 70°$ the informative Cr alloy is 26 μm and increases with angle widening). Therefore in the diffraction patterns the lines from the substrate are presented.

Fig. 4 shows the photographs of coated and uncoated tubes after oxidation in air for 3600 s at 1020 and 1100 °C.

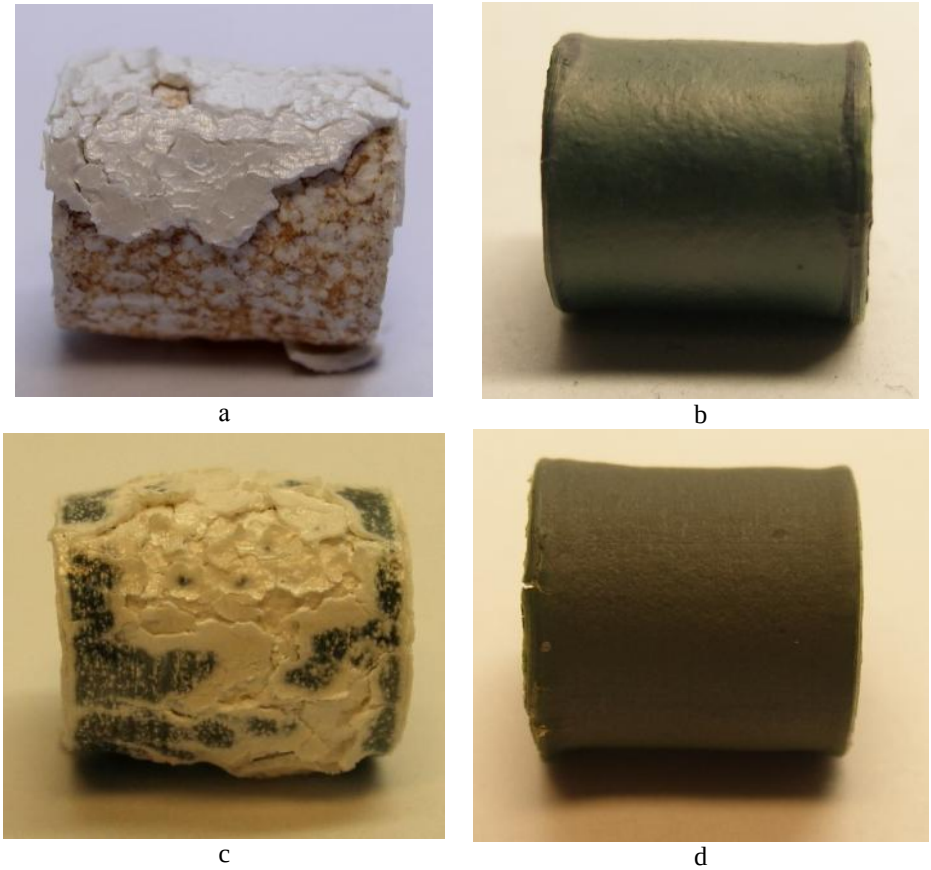

a b

c d

Fig. 4. Photographs of uncoated E110 tubes (a, c) and Cr-coated tubed (b, d) after oxidation in air at temperatures 1020 °C (a, b) and 1100 °C (c, d)

Uncoated samples are oxidized, cracked and, in some part, fractured. It is seen that the fracture at 1020 °C is more significant than at T = 1100 °C (see Fig. 4,a,c). Apparently, at T = 1100 °C the phase transition (α+β)→β occurs more quickly and causes minor fractures [17]. At the edges of coated samples the cracking marks are observed that is conditioned by the coating absence on the inner and end surfaces of tubes.

Figs. 5 and 6 present the micrographs of metallographic sections of oxidized E110 tubes with different magnification.

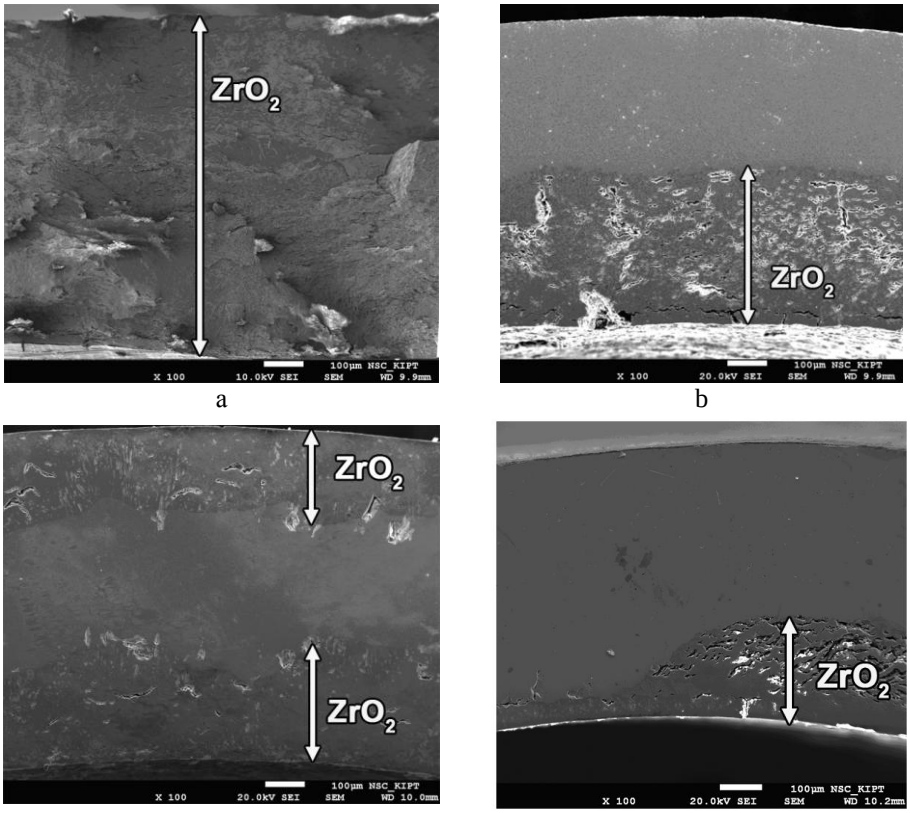

Fig. 5. Micrographs of metallographic sections of E110 tubes: uncoated (a, c) and Cr-coated (b, d) after oxidation at temperatures 1020 °C (a, b) and 1100 °C (c, d)

During oxidation at temperature of 1020 °C the uncoated tube oxidizes on the outer side throughout the wall thickness and cracks (see Fig. 5,a). Microprobe analysis data show that the oxygen concentration throughout the oxidized layer thickness makes 22 wt.%. The tube with a coating on the outer side oxidizes only on the inner side. The inner oxide layer thickness is near 300 μm, the pore size is ~ 5…20 μm. The cracks in the longitudinal direction at the depth of ~ 100 μm lead to the separation of the crumbling oxide layer from the denser inner layer (see Fig. 6,a). And the coating oxidized to depth less than 5 μm protects the zirconium alloy against the interaction with atmosphere (Figs. 6,b and 7,a).

As the oxidation temperature increases to 1100 °C the uncoated tube oxidation occurs on the both sides uniformly to depth of ~ 250 μm (see Fig. 5,c). The oxide layer contains also pores and cracks the sizes of which are from tens to hundreds of microns (see Fig. 6,c). The oxygen concentration in the oxide layer is within 22 wt. %, and in the central part it is near 5 wt.% that corresponds to the solid oxygen solution in zirconium.

The oxide layer thickness in the coating slightly increases but does not exceed its limits (see Fig. 6,d). According to the profile of element concentration, constructed by the microprobe analysis data (see Fig. 7,b), the oxygen concentration decreases from 30 to 4 wt. % in the ~ 6 μm surface layer of the coating. The process of chromium oxidation in air versus time obeys the parabolic law and is determined by the chromium cation diffusion through the Cr_2O_3 oxide layer [20]. In this experiment the oxidation duration was one hour and the oxide layer thickness in pure chromium was ~ 3 μm at 1000 ^oC and ~ 6 μm at 1110 ^oC.

Fig. 7,b show that at T = 1100 °C the chromium diffusion into the zirconium alloy increases. In [21] the increase of the rate of chromium diffusion into the zirconium alloy at this temperature was observed too.

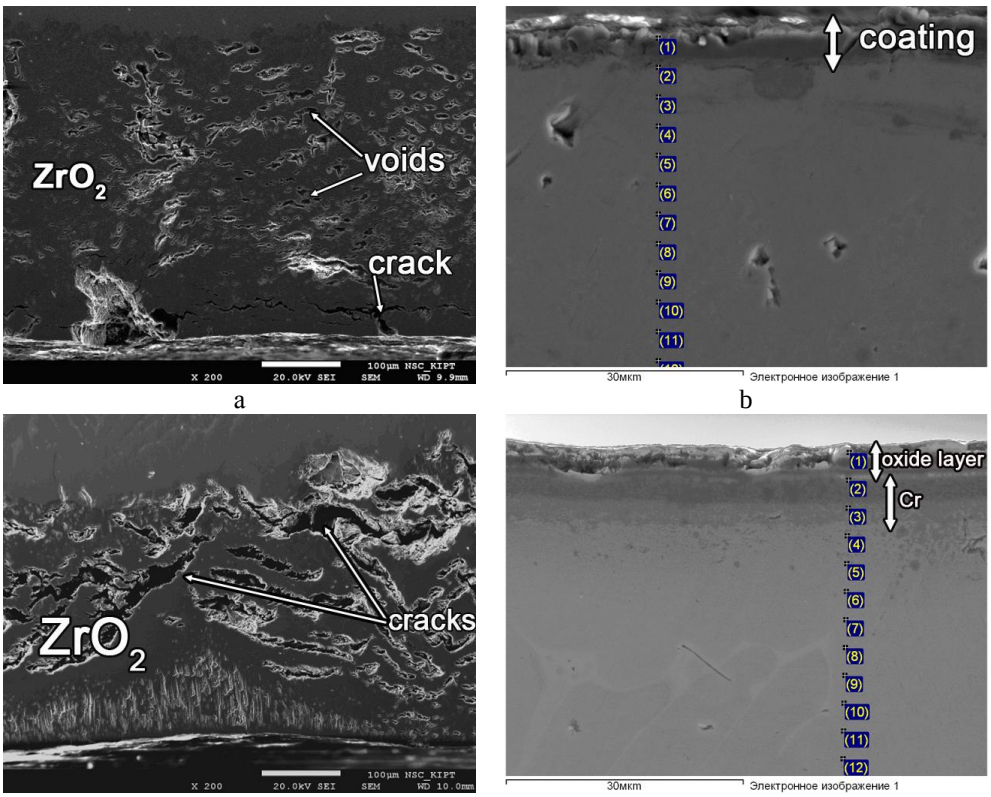

Fig. 6. Micrographs of oxidized layers on the metallographic sections of E110 tubes: uncoated (a, c) and Cr-coated (b, d) after oxidation at temperatures of 1020°C (a, b) and 1100°C (c, d)

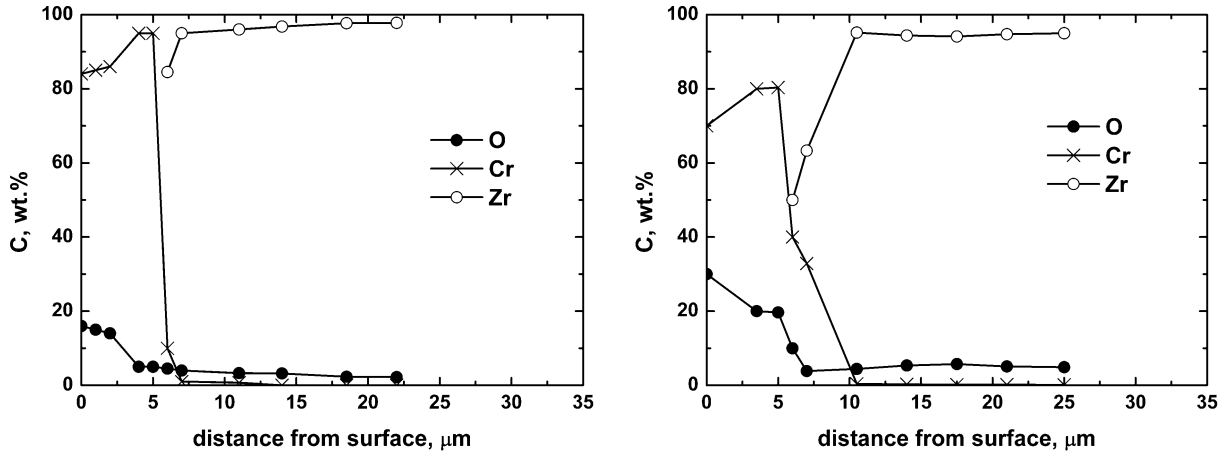

Fig. 7. Concentration of elements in the coatings of tubes after oxidation at temperatures 1020 °C (a) and 1100 °C (b)

The zirconium alloy oxidation is characterized by the change in its hardness. The indentation data show that the hardness of uncoated and coated tubes measured on the metallographic section along the tube radius has no difference on the inner and outer sides and equals to ≈ 2 GPa throughout the thickness. After oxidation at T = 1020 °C the Zr-1Nb nanohardness under the coating increases from 2 to 3.5 GPa. On the uncoated side the nanohardness of the whole oxidized layer is at a level of 12 to 14 GPa and reaches ~ 16 GPa at oxidation temperature T = 1100 °C. The nanohardness under the coating is unchanged.

The Cr-coated Zr samples were investigated with a diffractometer to determine their phase composition before and after oxidation. Table 1 presents the data on the phase composition and lattice parameters of the phases being observed. On the uncoated zirconium samples after oxidation at 1020 and 1100 °C a single-phase monoclinic zirconium oxide is formed (see Fig. 3,a). The α-ZrO_2 phase lattice parameters are slightly increasing at 1100 °C.

.

Phase composition and parameters of the samples being studied

Sample	T, °C	Phase Composition	Weight fraction, wt.%.	Phase lattice parameters
Zr initial	20	α-Zr	100	a=3,238 Å, c=5,150 Å
	1020	α-ZrO_2	100	a=5,140 Å; b=5,181 Å; c=5,332 Å; β=99,02°
	1100	α-ZrO_2	100	a=5,147 Å; b=5,195 Å; c=5,339 Å; β=99,04°
Zr+Cr	20	Cr	100	a=2,8847 Å
	1020	Cr	57,9	a=2,8847 Å
		Cr_2O_3	42,1	a=4,9618 Å; c=13,597 Å
	1100	Cr	57,6	a=2,8841 Å
		Cr_2O_3	42,4	a=4,9604 Å; c=13,586 Å

In the Cr-coated sample oxidized at T = 1020 °C (see Fig. 3,b) two phases are observed: besides chromium (weight fraction in the coating 57.9 wt.%) and chromium oxide Cr_2O_3 (weight fraction 42.1 wt.%). The chromium lattice parameter, is not changed as compared to the unoxidized coating, a=2.8847±2·10^{-4} Å. In chromium phase a texture (200) is observed with a degree of texturing of 63% that is much less than that in the unoxidized sample. In this phase a weak texture (110) is revealed with a degree of texturing of 17%. After oxidation at T = 1100 °C in the coating two phases are found (see Fig. 3,b): Cr (weight fraction in the sample is 57.6 wt.%) and chromium oxide Cr_2O_3 (weight fraction 42.4 wt.%). The chromium lattice parameter slightly decreased (Table). The texture (200) in the chromium phase is conserved and the degree of texturing decreased to 60%. In the Cr_2O_3 phase the texture (110) is enhanced and the degree of texturing is increased to 47%.

The oxidation tests of segments, cut from the uncoated zirconium alloy E110 fuel tubes, in air during one hour, have shown that at temperatures 1020 and 1100 °C their oxidation is catastrophic. Single-phase monocline ZrO_2 in the oxide layer is cracking and crumbling. On the tubes, with a protective vacuum-arc nonporous micro-crystalline chromium coating, in the upper coating layer of ~ 3…5 μm, the Cr_2O_3 oxide is formed preventing the oxygen to penetrate deep into the metal. At temperature of 1100 °C a rather strong diffusion interaction of the chromium coating with the zirconium substrate is observed. However, the X-ray analysis data show that the chromium phase in the coating is conserved. At high-temperature oxidation in air the chromium coating is a much more effective barrier against oxygen than the oxide layer formed on the alloy E110.

CONCLUSIONS

Steam-oxidation tests conducted with samples from E110 tubes permit to make the following conclusions:

1. The developed and investigated micro-crystalline (average grain size of ~ 450 nm) chromium coatings provide an effective protection of the alloy E110 against oxidation in air at T = 1020 °C for 3600 s.

2. During the tests at temperature of ≥ 1020 °C the strong oxidation of the alloy E110 occurs to the depth of ~ 250 μm with formation of a monocline crumbling ZrO_2 film while under the same conditions in the chromium coating a Cr_2O_3 oxide film is formed up to the depth of 5 μm.

3. Vacuum-arc chromium coatings of ~ 7…8 μm thickness serve as a protective barrier against the alloy E110 oxidation to temperature of 1100 °C during one hour since under the coating the substrate oxidation is not observed.

REFERENCES

1. C. Duriez, D. Drouan, G. Pouzadoux. Reaction in air and in nitrogen of pre-oxidised Zircaloy-4 and M5™ cladding // *Journal of Nuclear Materials.* 2013, v. 441, p. 84-95.

2. C. Duriez, T. Dupont, B. Schmet, F. Enoch. Zircaloy-4 and M5^{TM} high temperature oxidation and nitriding in air // *Journal of Nuclear Materials.* 2008, v. 380, p. 30-45.

3. Y. Yan, T.A. Burtseva, M.C. Billone. High-temperature steam-oxidation behavior of Zr-1Nb cladding alloy E110 // *Journal of Nuclear Materials*. 2009, v. 393, p. 433-448.

4. I.A. Petelguzov. Kinetics and mechanism of Zr1Nb alloy corrosion under steam heating in the temperature range from 660 to 1200 °C // *Voprosy Atomnoj Nauki i Tekhniki. Seriya "Fizika radiatsionnykh povrezhdenij i radiatsionnoye materialovedeniye" (89).* 2006. N 4, p. 97-103 (in Russian).

5. S.A. Nikulin, A.B. Rozhnov, V.A. Belov, E.V. Li, V.S. Glazkina. Influence of chemical composition of zirconium alloy E110 on embrittlement under LOCA conditions – Part 1: Oxidation kinetics and macrocharacteristics of structure and fracture // *Journal of Nuclear Materials.* 2011, v. 418, p. 1-7.

6. K. Sridharan, S.P. Harrington, A.K. Johnson, J.R. Licht, M.H. Anderson, T.R. Allen. Oxidation of plasma surface modified zirconium alloy in pressurized

high temperature water // *Materials and Design.* 2007, v. 28, p. 1177-1185.

7. Xinde Bai, Jian Xu, Fei He, Yudian Fan. The air oxidation of yttrium ion implanted zircaloy-4 at 500°C // *Nuclear Instruments and Methods in Physics Research B.* 2000, v. 160, p. 49-53.

8. Kurt A. Terrani, Chad M. Parish, Dongwon Shin, Bruce A. Pint. Protection of zirconium by alumina- and chromia-forming iron alloys under high-temperature steam exposure // *Journal of Nuclear Materials.* 2013, v. 438, p. 64-71.

9. Jeong-Yong Park, Il-Hyun Kim, Yang-Il Jung, Hyun-Gil Kim, Dong-Jun Park, Byung-Kwon Choi. High temperature steam oxidation of Al3Ti-based alloys for the oxidation-resistant surface layer on Zr fuel claddings // *Journal of Nuclear Materials.* 2013, v. 437, p. 75-80.

10. I.A. Petelguzov. Influence of protective aluminum and chromium coatings on the oxidation of zirconium and zirconium alloys // *Voprosy Atomnoj Nauki i Tekhniki.* 2012, N 2(78), p. 114-119 (in Russian).

11. A.S. Kuprin, V.A. Belous, V.N. Voyevodin, V.V. Bryk, R.L. Vasilenko, V.D. Ovcharenko, G.N. Tolmachova, P.N. Vygov. High-temperature air oxidation of E110 and Zr-1Nb alloys claddings with coatings // *Problems of Atomic Science and Technology. Series* "*Vacuum, Pure Materials, Superconductors".* 2014, N 1, p. 126-132.

12. I. Idarraga-Trujillo, M. Le Flem, J.-C. Brachet, M. Le Saux, D. Hamon, S. Muller, V. Vandenberghe, M. Tupin, E. Papin, E. Monsifrot, A. Billard, F. Schuster. Assessment at CEA of coated nuclear fuel cladding for LWRS with increased margins in LOCA and beyond LOCA conditions // (*Conference Paper) LWR Fuel Performance Meeting, Top Fuel 2013*. 2013, v. 2, p. 860-867.

13. Hyun-Gil Kim, Il-Hyun Kim, Yang-Il Jung, Dong-Jun Park, Jeong-Yong Park, Yang-Hyun Koo. High-temperature oxidation behavior of Cr-coated zirconium alloy // *Ibid*, p. 842-846.

14. A.N. Rakitskii, V.I. Trefilov. Optimum alloying of chromium with highly active elements. A survey // *Soviet Powder Metallurgy and Metal Ceramics*. 1977, v. 16, issue 9, p. 703-711.

15. V.F. Gorban', N.I. Panarina, A.N. Rakitsky. Heat-resistance of gas-thermal chromium-base materials // *Zashchita metallov*. 1994, v. 30, N 6, p. 596-598 (in Russian).

16. V.I. Trefilov, V.F. Zelensky, V.S. Krasnorutsky, A.N. Rakitsky, V.S. Pavlov, V.A. Pisarenko, Yu.I. Rogovoj, E.V. Turtsevich, V.F. Gorban'. Developing and testing the UO_2-Cr dispersion fuel for high-temperature fast neutron reactors // *Proceedings of the International Conference "Radiation Materials Science".* Kharkov: KIPT, 1991. v.8, p. 103-111 (in Russian).

17. N.I. Ishchenko, I.A. Petelguzov, E.A. Slabospitskaya, R.L. Vasilenko. Influence of high-temperature steam annealing on the structure of Zr-1Nb fuel elements // *Voprosy Atomnoj Nauki i Tekhniki. Seriya "Fizika radiatsionnykh povrezhdenij i radiatsionnoye materialovedeniye (88)".* 2005, N 5, p. 115-120 (in Russian).

18. . I.I. Aksenov, A.A. Andreev, V.A. Belous, V.E. Strel'nitskij, V.M. Khoroshikh. *Vacuum arc. Plasma sources, coatings deposition, surface modification.* Kyiv: "Naukova dumka", 2012, 728 p.

19. W.C. Oliver, G.M. Pharr. Measurment of hardness and elastic modulus by instrumented indentation: Advances in understanding and refinements to methodology // *J. Mater. Res.* 2004, v. 19, N 1, p. 3-20.

20. Kaori Taneichi, Takayuki Narushima, Yasutaka Iguchi, Chiaki Ouchi. Oxidation or nitridation behavior of pure chromium and chromium alloys containing 10 mass% Ni or Fe in atmospheric heating // *Materials Transactions.* 2006, v. 47, N 10, p. 2540-2546.

21. G.M. Hood. Point defect diffusion in α -Zr // *J. Nucl. Mater.* 1988, v. 159, p. 149-175.

Article received 05.02.2015

ВАКУУМНО-ДУГОВЫЕ ХРОМОВЫЕ ПОКРЫТИЯ ДЛЯ ЗАЩИТЫ СПЛАВА Zr-1Nb ОТ ВЫСОКОТЕМПЕРАТУРНОГО ОКИСЛЕНИЯ НА ВОЗДУХЕ

А.С. Куприн, В.А. Белоус, В.В. Брык, Р.Л. Василенко, В.Н. Воеводин, В.Д. Овчаренко, Г.Н. Толмачёва, И.В. Колодий, В.М. Лунёв, И.О. Клименко

Изучено влияние вакуумно-дуговых покрытий из Cr на стойкость сплава Э110 к окислению на воздухе при температурах 1020 и 1100 °C в течение 3600 с. Методами сканирующей электронной микроскопии, рентгеноструктурного анализа и наноиндентирования исследованы толщина, структура, фазовый состав, механические свойства покрытий и оксидных слоёв. Показано, что покрытие из хрома служит эффективной защитой твэльных трубок от высокотемпературного окисления на воздухе в течение часа. В покрытии при окислении (T = 1100 °C) формируется оксид Cr_2O_3 толщиной ~ 5 мкм, который препятствует дальнейшему проникновению кислорода под покрытие, форма трубок сохраняется. Трубки без покрытия при этих испытаниях окисляются с образованием пористого моноклинного оксида ZrO_2, толщина которого ≥ 250 мкм, образцы деформируются, происходит растрескивание и отслоение оксидного слоя.

ВАКУУМНО-ДУГОВІ ХРОМОВІ ПОКРИТТЯ ДЛЯ ЗАХИСТУ СПЛАВУ Zr-1Nb ВІД ВИСОКОТЕМПЕРАТУРНОГО ОКИСЛЕННЯ НА ПОВІТРІ

О.С. Купрін, В.А. Білоус, В.В. Брик, Р.Л. Василенко, В.М. Воєводін, В.Д. Овчаренко, Г.М. Толмачова, І.В. Колодій, В.М. Луньов, І.О. Кліменко

Вивчено вплив вакуумно-дугових покриттів із Cr на стійкість сплаву Е110 до окислення на повітрі при температурах 1020 та 1100 °С протягом 3600 с. Методами скануючої електронної мікроскопії, рентгеноструктурного аналізу та наноіндентування досліджені товщина, структура, фазовий склад, механічні властивості покриттів та оксидних шарів. Показано, що покриття з хрому слугують ефективним захистом твельних трубок від високотемпературного окислення на повітрі протягом години. В покриттях при окисленні (Т = 1100 °С) формується оксид Cr_2O_3 товщиною ~ 5 мкм, який перешкоджає подальшому проникненню кисню під покриття, форма трубок зберігається. Трубки без покриття при цих випробуваннях окисляються з формуванням пористого моноклінного оксиду ZrO_2, товщина якого ≥ 250 мкм, зразки деформуються, виникає розтріскування та відшарування оксидного шару.